Experimentally validation and vibro-acoustic modeling of 3D bio-printed grafts for potential use in human tympanic membrane regeneration

Ali A. Rostam-Alilou, Hamid Jafari, Ali Zolfagharian, Ahmad Serjouei, Mahdi Bodaghi

PII: S2405-8866(21)00059-2

DOI: https://doi.org/10.1016/j.bprint.2021.e00186

Reference: BPRINT 186

To appear in: *Bioprinting*

Received Date: 8 November 2021

Revised Date: 8 December 2021

Accepted Date: 13 December 2021

Please cite this article as: A.A. Rostam-Alilou, H. Jafari, A. Zolfagharian, A. Serjouei, M. Bodaghi, Experimentally validation and vibro-acoustic modeling of 3D bio-printed grafts for potential use in human tympanic membrane regeneration, *Bioprinting* (2022), doi: https://doi.org/10.1016/j.bprint.2021.e00186.

CRediT authorship contribution statement:

Ali A. Rostam-Alilou: Conceptualization; Methodology; Investigation; Visualization; Formal analysis; Validation; Writing and Editing – original draft.

Hamid Jafari: Methodology; Investigation; Visualization; Formal analysis; Validation, Data curation; Editing – original draft.

Ali Zolfagharian: Methodology; Investigation; Formal analysis; Supervision; Editing – original draft.

Ahmad Serjouei: Methodology; Investigation; Formal analysis; Supervision; Editing – original draft.

Mahdi Bodaghi: Conceptualization; Methodology; Investigation; Formal analysis; Supervision; Project administration; Writing and Editing – original draft.

Experimentally validation and vibro-acoustic modeling of 3D bio-printed grafts for potential use in human tympanic membrane regeneration

Ali A. Rostam-Alilou [a], Hamid Jafari [a,b], Ali Zolfagharian [c], Ahmad Serjouei [a], Mahdi Bodaghi [a] *

[a] Department of Engineering, School of Science and Technology, Nottingham Trent University, Nottingham NG11 8NS, United Kingdom
[b] Mechanical Engineering, University of Tehran, Tehran, Iran
[c] School of Engineering, Deakin University, Geelong 3216, Australia

ARTICLE INFO

Keywords:
Tympanic membrane
3D Bioprinting
Dynamic modeling
Vibro-acoustic analysis
Computational validation
Tissue Engineering

ABSTRACT

Three-dimensional (3D) bioprinting is a pioneering field of tissue engineering obtaining a special role in most medical engineering fields. Otology is a medicine branch that needs bio-printing technology to receive aids for the reconstruction of aesthetic necessities of the ear and treating hearing loss diseases due to several pathological reasons such as tympanic membrane (TM) perforation. In this work, computational dynamic simulations of 3D printed TM grafts are presented. The main purpose of numerical modeling of these experimentally validated composite scaffolds is to demonstrate the worth of simulation in shortening the design time and decreasing testing costs of biomedical engineering projects. The simulated 3D printed TM grafts were fabricated in two main architectural categories using three different polymeric materials of polydimethylsiloxanes (PDMS), flex polylactic acid (PLA), and polycaprolactone (PCL) with uniform infilling of fibrincollagen composite hydrogels. As a numerical and dynamic validation study, firstly, a finite element (FE) simulation of the artificial TM grafts is carried out for a vibro-acoustic analysis by the COMSOL Multiphysics software package. Then a comparative study of results obtained from the dynamic modeling is performed with a set of existing data taken from experimental validation test results from digital optoelectronic holography (DOEH) and laser Doppler vibrometry (LDV). Observations show a good correlation between the acoustic behaviors of in vitro tested 3D printed TM grafts and computational models in both frequency domain motion and normalized velocity patterns. Satisfying correlation between acoustic properties of simulated TM grafts and experimental test results shows potential applications of printed TM grafts in tympanoplasty.

1. Introduction

Tympanic membrane (TM), or eardrum, is a thin and resilient membrane with a total thickness in the mean value of 74 μm [1], located into the middle ear. It contains a lateral cutaneous layer, intermediate fibrous layer, and medial mucus layer [2]. The TM captures acoustic energy from the environment and transmits it to the ossicular chain of the middle ear as a vibration response to start the hearing procedure. Sometimes appearing an injury by a group of middle ear diseases such as otitis media and/or traumatic perforation [3], injuries by externally applied stresses like blast-induced loads [4] etc., in TM may lead to hearing loss and recurrent infections. But the TM perforation is known as the most prevalent problem. Besides, middle ear infections, postoperative complications, and traumatic rupture because of increased pressure are the most common causes of TM perforation [5,6]. Although TM has an auto-regenerative feature, intensive perforations need to be reconstructed by surgical approaches with various materials such as autologous tissue, fascia, cartilage, fat, or perichondrium. Additionally, two standard therapeutic methods of myringoplasty (also called type 1 tympanoplasty) and tympanoplasty are used for restoring damaged TM. These methods despite high success rates, have some limitations and drawbacks as well. Myringoplasty is a surgical procedure using multiple autologous grafts, allografts, and synthetic grafts for repairing TM. These techniques are based on the use of grafts to repair the perforation of TM [7] but they are faced with particular performing challenges. Thus, the needing for low-cost, non-surgical, and more reliable alternatives to hearing loss treatment encourages researchers to focus on finding novel approaches such as growth factors, cells, and artificial scaffolds [8]. The possible donor site morbidity, lacking transparency, vibration at lower amplitudes, acoustic implications, air-dried characteristics, re-perforation of TM, and other operating special assignments are typical limitations of existing grafts [9]. As a result, because of the mentioning limitations, tissue engineering can provide promising alternatives for the surgical treatment of hearing diseases [10]. An optimum and robust model of the grafts needs to be developed and studied considering essential bioengineering aspects. Tissue engineering undoubtedly plays a significant role in filling existing gaps between medical problems and engineering solutions. Besides all these, finding a novel and more applicable method to build an artificial and TM structure-inspired model is necessary to struggle with major defects of existing methods. On the other hand, during the last decade, three-dimensional (3D) bioprinting of smart multi-materials for tissue regeneration [11] and tissue scaffolds appeared pioneering method in medical engineering [12,13]. In general, precise complex design, loading cells and bioactive molecules, and creating tissue-like structures are three main advantages of 3D bioprinting, while finding a suitable biomaterial for printing scaffolds is a real known challenge [14]. Although tissue engineering of human TM is a young field of study in hearing research and bioprinting, some researchers tried to develop novel and reliable methods for use in different areas of otology such as ossiculoplasty (repairing ossicular chains), myringoplasty, and tympanoplasty with the aid of biomaterial-based prostheses [15–17] and templates [18]. For illustration, employing 3D printing technology to produce artificial eardrum patches for the treatment of TM perforations as scaffolds with polylactic acid, Chitosan (CS), and Sodium Alginate (SA) was carried out by Ilhan et al. [19]. Their model has potential use as an alternative to surgical treatment or paper patch. Inspiring the patching technology in TM repairing, Kim et al. [20] studied a novel

*Corresponding author:
Email address: mahdi.bodaghi@ntu.ac.uk

transparent duck's feet collagen film patch with the demonstration of its biocompatibility and biodegradability as a good biomaterial-based option for TM patching procedure [20]. But for the first time, Kozin et al. [21] used 3D printing technology to design, fabrication, and bio-printing of polymeric TM grafts. Their studying target was supported by printing TM grafts in two main architectural categories of 8 and 16 circumferential and radial filaments. They also used multi-material of flex-polylactic acid (PLA), polydimethylsiloxanes (PDMS), and polycaprolactone (PCL) to fabricate the scaffolds (see Figure 1). The main reasons for selecting these materials are their unique polymeric properties for biomedical applications. For example, the suitable elastic property of PDMS from the Si-O structure makes it a more flexible material than other polymers. Furthermore, by having a good elasticity characteristic, PDMS can stretch and release its tension to return to its initial state when subjected to a tensile force. In addition, the PCL polymer contains desirable physical and mechanical properties with high flexibility. Because of this, it has attracted particular attention in biomedical and bioprinting applications during the last years. Furthermore, by having a relatively high melting point (~200 °C) [22] and because of being readily melt-spinnable and stress crystallizes upon drawing, the PLA plays a significant role in manufacturing some essential components such as fibers and films [23]. PLA allows cell adhesion but because it is not bioactive, it does not support cellular activity. Also, the empty space among filaments was filled with uniform infilling of fibrincollagen composite hydrogel. They tested the printing samples by digital optoelectronic holography (DOEH) and laser Doppler vibrometry (LDV) for in-vitro acoustic and mechanical evaluation. The feasibility of 3D printed TM grafts in reflecting sound-induced motion patterns of the human TM and also improving resistance to deformation compared to temporalis fascia was investigated. Also, for experimental validation of their studies, they examined the 3D printed grafts with a comparative analysis among three groups of corresponding samples, temporalis fascia, and human TM (for observation of dynamic responses). Their studies showed that the resistance of 3D printed grafts to deformation was at a considerable level compared to temporalis fascia. This was a promising result demonstrated that 3D printed TM grafts were feasible for repairing perforated human eardrums. But further studies considering the other bioengineering aspects are yet to be conducted.

In this study, a numerical and computational validation of the TM grafts is performed to support experimental studying for the design and fabrication of TM grafts by bioprinting technologies. Furthermore, the investigation aims to apply multi-physical modeling techniques to shorten the designing and pre-studying steps of the 3D printing procedure of optimized TM grafts. To perform this study, in the first step, the finite element modeling (FEM) of the printed grafts is carried out by COMSOL Multiphysics software package according to the architectural and material properties mentioning in related literature of [21]. Then simulation results are taken under a comparative and statistical analysis to find the correlation between existing experimental data reported by experimental studies and simulation results obtaining from this work.

2. Materials, Geometrical Characteristics, and Method

2.1. Materials

Different materials are used as printing biomaterials in surgical and other biomedical applications such as polymers, metals, and ceramics. Exploration of an ideal material for grafts is one of the significant challenges in TM reconstruction. Materials such as autologous grafts (using autologous muscle in musculoplasty), homografts (harvested from other humans), xenografts (harvested from animals), and synthetics are used for TM repair. In general, trying to find a more suitable material for TM repair and graft manufacturing is continuing by researchers yet. Scientists believe that the novel materials should be easy to obtain and fashion, available in high quantities with a low price, have a significant level of safety, show no interference in-ear components to disrupt the hearing process, and cause no cosmetic changes [24]. These are the minimum criteria that the corresponding material would satisfy. However, it is demonstrated that polymers because of their biodegradability, efficiently processing, and applicability characteristics, play a unique role in bioprinting and tissue engineering [25]. The under studying TM grafts in this project were 3D printed using different synthetic polymers of PDMS, PCL, and flexible PLA.

PDMS is non-toxic with good biocompatibility and biostability silicone elastomer [26]. It is widely used in a variety of medical implants. The hyperelastic behavior of this material helps it to undergo large deformations without early rupture [27]. In addition, because of being an acoustically isotropic polymer, it is a suitable candidate for biomedical studies like ultrasound, acousto-fluidics, and tissue fabrication [28]. This may be one of the main reasons to select this material for designing TM grafts.

Besides, the biodegradability character of PLA and PCL thermoplastic polymers has listed them among the group of polymeric inks in 3D printing. PLA and PCL are used not only for bioprinting applications but also for drug delivery, bone regeneration [29], and dermal scaffold and human skin-based projects [30]. PCL also has high solubility and combination characteristics with other polymers as a biodegradable, hydrophobic, and semi-crystalline polymer. Mentioned specifications, low speed of degradation, and superior rheological properties are adequate reasons to introduce PCL as a suitable alternative for graft designing [31]. But PLA is a linear aliphatic polymer that is obtained special attention in biomedical applications with replacing conventional petrochemical-based polymers in industry. Having good mechanical properties such as high strength, biocompatibility, stiffness, and thermoplasticity [32], but lower compressive strength and tending to be brittle, low cost, renewable feedstocks, and easy processability are the other characteristics of PLA. This polymeric material is one of the known materials suitable for fused deposition modeling (FDM) [33] that is the most applicable method in 3D printing of thermoplastic polymers [34]. In contrast, PCL is not only a suitable choice for melt-based extrusion printing due to consisting considerable rheological and viscoelastic properties but also shows excellent stiffness and extended degradation after printing. This feature makes it useful mostly for complex tissue engineering and applications [35]. Generally speaking, the structural performance of polymeric scaffolds may have a dependence on parameters like manufacturing temperature, printing speed and orientation, and the layer thickness of the filaments [36].

According to the numerical simulation requirements and mentioned materials for fabrication of the corresponding TM grafts by Kozin et al. [21], the acoustic and mechanical properties of PDMS, PLA, and PCL are extracted using several pieces of literature [28,31,37]. For performing FEM simulation, the summary of these properties is collected in Table 1.

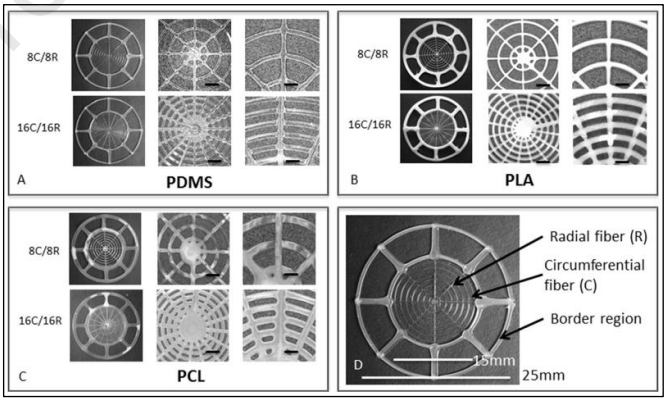

Fig. 1. 3D printed TM grafts geometrical properties: (A-C) Images of TM scaffolds composed of PDMS, PLA, and PCL filaments, respectively, with 8C/8R and 16C/16R filamentary architectures. The TMs in the first column of each box have a total diameter of 25 mm. The following two columns show higher magnification images, 50 with a scale bar of 1 mm and 100 with a scale bar of 500 mm, respectively: (D) Image of a representative printed scaffold highlighting design features (reprinted and modified from [21] with permission from Elsevier).

Table 1
Summary of basic acoustic properties of three polymers used in simulation

Materials	Properties	
	Mass Density (gr/cm3)	Bulk Sound Speed (m/s)
PDMS	1.03	1076.5
PLA	1.14	1250
PCL	1.20	1150

Table 2
Summary of geometrical properties of 3D printed TM grafts

TM Grafts	Dimension		
	Width (mm)	Supporting border (mm)	Thickness (μm)
PDMS	15	10	209 ± 9
PLA	15	10	215 ± 8
PCL	15	10	246 ± 15

2.2. Geometrical properties of 3D printed TM grafts

For inspiration of designing architecture, scanning and transmission electron microscopy images of the human TM were used by designers [21]. As mentioned before, 3D printed TM grafts were designed using three different materials, namely PDMS, PLA, and PCL in two separate filament groups categorized by circumferential [C] and radial [R] fibrous arrangements. These filament groups were chosen in two architectural categories with 8 filaments (8C/8R) and 16 filaments (16C/16R) for evaluation (see Figure 1). Although the geometrical properties of the grafts play a significant role in the structural and acoustic behavior, the radial lattice patterns in two categories are selected for the morphological design of bio-printed grafts. The potential use and feasibility of lattice structures in 3D bioprinting of artificial scaffolds for TM regeneration are demonstrated in our previous study [38]. All printed grafts were in an intrinsic fibrous structure with a standard measure of 15 mm diameter and an additional 10 mm border region for supporting during in-vitro testing. As shown in Table 2, the samples were in similar geometrical properties except for thickness. That difference was appeared due to the impact of variation of thickness in the printing process. Optical microscopy coupled with image analysis using Image J software and a micrometer were used for determining the filament widths and thicknesses, respectively.

2.3. Method

The numerical simulation of multiphysics models helps to observe expected results before in vivo and in vitro proceedings. FEM modeling and studying prosthesis before surgery [39,40], human organ systems [41], and other applied simulations are many examples of employing numerical studies in biomedical engineering. The simulation, analysis, and results exposition procedure are performed following three main steps, as shown in Figure 2. In this study, the modeling is carried out by the finite element analysis tool of the COMSOL Multiphysics Software package. The material properties of corresponding TM graft models are assumed similar to the experimental tested models. PDMS, PLA, and PCL are assigned to the TM graft filaments. The infilling areas are also modeled by fibrin/collagen hydrogel matrix. FEM models are simulated with geometrical characteristics shown in Figure 3, again in two architectural categories of 8C/8R and 16C/16R. 3D printed scaffolds are simulated according to the details presented earlier in Table 1 for material properties and in Table 2 for geometrical information to obtain more accurate results. Different mesh types are used to simulate the FE model. The mesh convergence is evaluated for these models, and the acceptable mesh type has a good fit in this finite element modeling.

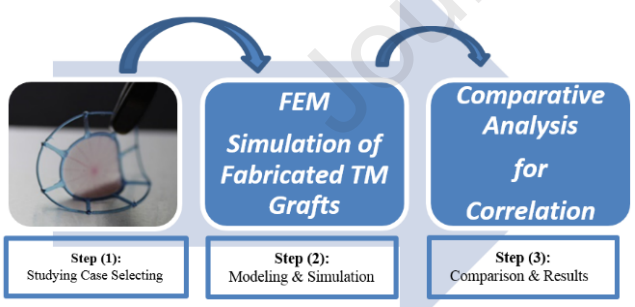

Fig. 2. Studying method and following steps for simulation of the TM grafts

In general, the fine size is recognized as a more suitable meshing method for the models. The meshing is also configured with the triangular element type including three nodes and three sides for generation supporting points in two degrees of freedom. Based on the physics of the pressure acoustics study, using triangular elements has been recommended by previous studies [42]. The overall number of elements and the mesh size is controlled according to the physics-controlled mesh sequence type. This limits the maximum element size to a range less than ((wave length)/5). So, the 1.68 mm is calculated for the maximum size of the elements for the models. For carrying out the frequency-domain analysis, an acoustic module of the Pressure Acoustics Frequency Domain (ACPR) interface has been created in COMSOL. As the ACPR is an appropriate module for studying acoustics-related phenomena without involving a liquid. But, also for analysis of the discrepancies between different pressure variations to observe the diffusion of acoustic waves on a model into a liquid environment, ACPR may be a suitable module. This method operates as a physics interface by solving the Helmholtz equation for given frequencies. Besides, the sound hard boundary (SHB) and the other initial values are assigned to the nodes for the creation of an acoustic environment along with acoustic loading according to the experimental test details. Considering the ACPR multiphysics requirements, the outer border region of the graft models (inspired by the natural behavior of the human TM) is restricted by the boundary conditions [38].

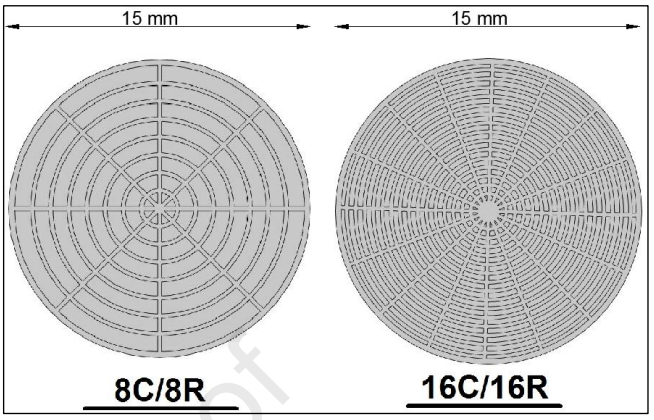

Fig. 3. Geometrical properties of FEM simulated grafts in two main categories of 8C/8R and 16C/16R (without outer border).

3. Vibro-acoustic Analysis and FEM Simulation

Demonstration of the acoustic properties of printed TM grafts is carried out by designers before and the experimental validation results summary is presented in section 3.1. according to [21]. As mentioned earlier, they performed DOEH and LDV experimental tests to show the potential application of printed TM grafts in tympanoplasty. In this research, a numerical modeling of the 3D printed TM grafts is carried out to find the correlation between the computational simulation and reported experimental investigation results. However, two main demonstration factors of displacement measurement and velocity variation of tested surfaces were experimentally validation. But to support these results, plotting the FEM acoustic analysis outputs are performed according to the material and geometrical properties. Then, the comparative analysis is done to discuss similarities and/or differences. For referring validated results, a brief of the experimental test reported by Kozin et al. [21] is presented in the next section.

3.1. Experimental test results summary

Series of numerical and graphical data were collected by Kozin et al. [21] according to their experimental studies on human temporalis fascia and tympanic membrane. They were prepared the samples harvested from the fresh cadaveric regions by a surgical procedure. The results were reported by carrying out comparative analysis to observe a primary evaluation and structural-acoustic performance (using DOEH) of grafts design. Despite many limitations include natural differences in loading and morphology in the middle ear, the expected correlation was observed between samples and the reference data. The loading on the samples was applied as continuous sound pressure at the four different frequencies of 400, 1000, 3000, and 6000 Hz into the human hearing range with levels of the sound in accordance with the linear response limitation of the human natural TM. The mentioned sound pressure level (SPL) was selected from 80 dB to 110 dB to provide DOEH measurable edges on the surface of the sample. On the other hand, the LDV test was carried out to measure the velocity in the sample`s surface. Hence, displacement magnitudes and phase angles were provided as color mapping outputs for comparative analysis among TM grafts, the natural human TM, and fascia to validate the results. To obtain a close correlation between the maximum graft displacement magnitude obtained from DOEH and the delivered pure tone frequency the Spearman correlation test was applied with a type (I) error threshold of 0.05. According to the representation color maps, the main section of the experimental validation of samples specified in the comparative analysis. Reporting obtained results for more than 400,000 points on the surface of the printed grafts, fresh human TM sample, and temporalis fascia was the main output of their tests. According to the reported results, the TM composite grafts showed similar sound-induced motion patterns in all three materials. But there were also considerable differences in the amount and the place of the local maximum displacements. This was obvious at the

higher frequencies. But for displacement magnitudes, variable normalized displacements were reported among the three TM grafts. According to the experimental test results, the highest amount for mean maximum displacement was recorded at 400 Hz over the samples. Where, the greatest number for displacement magnitude was obtained for PLA printed grafts, followed by PCL and PDMS. In contrast, the smaller amount was recorded by PDMS consistently. While this was demonstrated that TM scaffold printing material had a vital role in studying maximum displacements, the filamentary arrangement, (8C/8R versus 16C/16R) had no significant impact on averaged maximal graft displacement. The most obvious observation was the inverse correlation between the maximum displacement and frequency for the natural human TM, printed grafts, and temporalis fascia. The notable feature of the DOEH is having limitations in frequency resolution despite providing high-resolution images from the membrane surfaces. For measuring the samples'

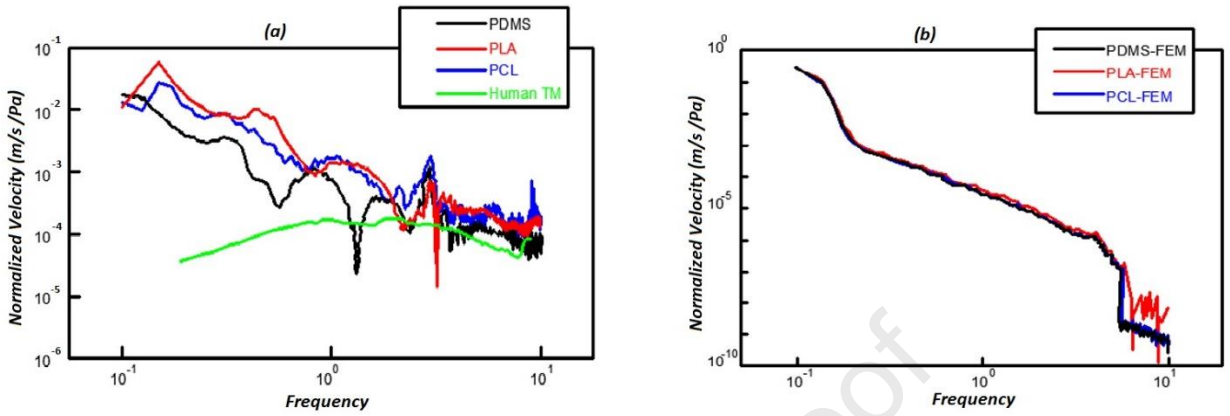

Fig. 4. Normalized velocity changes: a) normalized velocity by stimulus sound pressure of tympanic membrane composite grafts of varying composition (PDMS, PLA, and PCL), fascia and human TM measured by Laser Doppler vibrometry [21], b) recorded normalized velocity resulted from vibro-acoustic FEM simulated composite grafts

sound-induced velocity, LDV was employed to determine the normalized velocity in the printed grafts and the other samples. For another controlling aspect of surface velocity, the results obtained from LDV tests are presented in Figure 4a. These data were collected as normalized velocity by stimulus sound pressure of three materials composition bio-printed grafts, human natural TM, and fascia. It can be seen that the velocities of bio-printed grafts from three different materials of PLA, PCL, and PDMS with 8C/8R configuration were in a range of simultaneous peaks in the experiment frequency range. The highest velocity is seen at the lowest frequencies and appeared to peak close to 140 Hz at (0.08 m/s/Pa). Observations showed that the grafts made by PDMS exhibit low amounts of velocity and displacements. The difference between the mean velocity of the human fascia and printed grafts was observed from the LDV output data. The similarity in LDV velocity pattern and shape at high frequency was seen between human fascia and averaged composite grafts. Hence, the velocity at the middle of fascia and TM grafts was nearly equal to umbo velocity at the mid and high frequencies. As a result, a clear similarity in acoustic properties was exhibited by unloaded grafts compared to the human intact TM at mentioned frequencies. By comparing bio-printed TM grafts in different geometrical properties (in the filament feature aspect), it was obvious that the filament count was not effective in the general unity. Mechanical characteristics of the samples were also studied by dynamic mechanical analysis testing. Printing filament material was the significant factor that affected the revealed variable strength and amount of deformation testing on fascia and TM composite grafts. The highest load required by PCL was observable, followed by PLA and PDMS. Also, greater strength to stress was related to the PLA material-based grafts.

Consequently, with a brief review of reported data from the related literature, some key results can be summarized about experimental testing and validation of bio-printed TM composite grafts as follows:

1. Sound-induced motion patterns were in a good correlation in all three materials of bio-printed TM grafts.
2. The three TM composite grafts showed variable normalized displacement magnitudes.
3. The simple holographic motion (at lower frequencies) including complex patterns (at frequencies higher than 1000 Hz) was demonstrated for printed TM grafts.
4. PLA exhibited the most significant displacement magnitude at all frequencies while the smaller amount was related to PDMS.
5. The filamentary arrangement, (8C/8R and 16C/16R) was not a significant factor in averaged maximal graft displacement measures.
6. The inverse correlation in frequency and maximum displacement was observed for each of the natural human TM, bio-printed grafts, and fascia.
7. The grafts made by PDMS exhibited the lowest velocities with the lower displacements.
8. The lowest velocity was recorded for umbo at frequencies (< 1 Hz). So, the nearest sameness to umbo velocity at mid and high frequencies was also observed at the middle of the bio-printed grafts and fascia.
9. Temporalis fascia and the printed composite grafts had equal velocity.
10. At mid and high frequencies, unloaded grafts and human TM showed the same acoustic performance.
11. The filament count of the graft scaffolds did not affect the general sameness of the samples performance pattern.
12. In comparison with the bio-printed composite grafts, the temporalis fascia showed a low level of stability during mechanical tests.
13. Considerable strength to stress feature of the PLA-based grafts was observed in contrast to the other polymeric grafts.

3.2. Vibro-acoustic analysis results

3.2.1. Normalized surface motion of samples

Fabricated TM composite grafts based on PDMS, PLA, and PCL materials are simulated to evaluate the mechanical and acoustic behaviors of the grafts in frequency domain analysis. Adjustment of the existing data taken from related literature in an equal unite (frequency – dB) and range of data with computational analysis outputs is considered in the first step. Then color maps to explain the obtaining results from the vibro-acoustic analysis are constructed in a comparative analysis format. The color mapping for experimental tests is taken from [21]. An overall adjudication on the relationship between the performance of the fresh human TM and the printed TM grafts is an affirmative correlation. But for clarifying the real correlations between vibro-acoustic behavior patterns of human TM and simulated TM grafts, the most correlated regions are mentioned with the dashed lines in the corresponding FEM model results. These areas show a correlation between 80% to 90% in comparison with the human TM pattern in the same frequency domain. Figure 5 shows both experimental and numerical acoustic analysis results for all printed TM grafts, new human temporalis fascia, and human tympanic membrane (control samples) as displacement patterns. The mentioned data is related to the PDMS-based models for reporting normalized displacement amounts in sound pressure with the (dB re 1 μm/Pa) unit for different frequencies of 0.4, 1, 3, and 6 kHz. Where each column shows the changes taken from FEM analysis in the corresponding domain as standardized color bars according to the ODEH test mapping and outputs. In general at the higher frequencies, the printed PDMS material grafts show a high degree of homogeneity in radial bars of visual mapping. It can be seen that filaments geometrical features have no real impact on the final results. But it is undeniable that for PDMS material, correlation of obtained results for 8C/8R grafts is close to the DOEH results of the human TM. This is a significant observation where frequencies (< 3000 Hz) presented results related to 16C/16R do not show considerable homogeneity. Both architectural

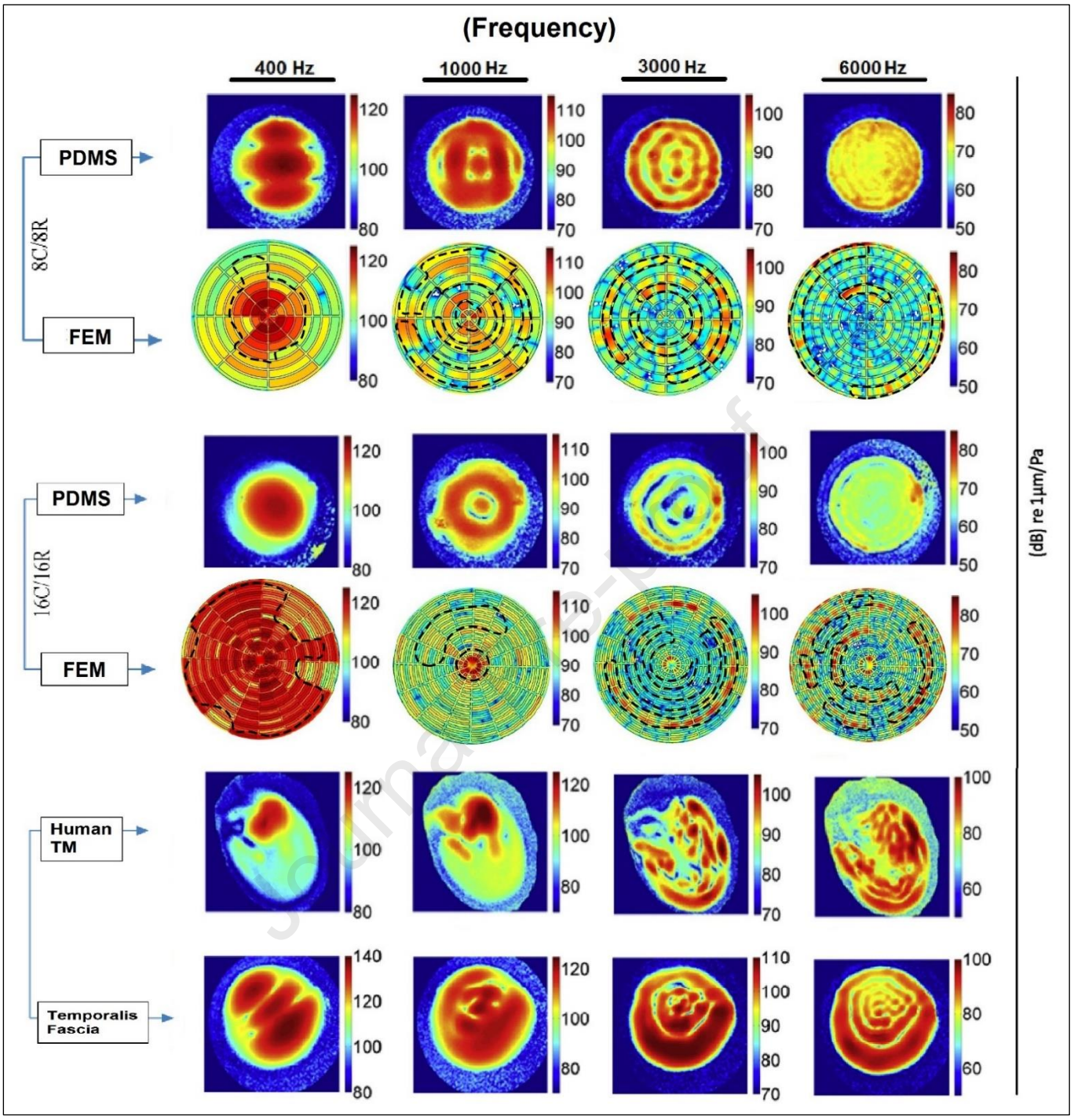

Fig. 5. Analysis results as normalized displacement by sound pressure at dB re 1 µm/Pa units for PDMS-based samples to provide data for comparative analysis with DOEH fringe patterns of printed tympanic membrane composite grafts (reprinted and modified from [21] with permission from Elsevier), and FEM models controlled with human tympanic membrane: Top two rows show the displacement patterns of the visible 9 mm diameter section of an 8C/8R filaments graft and FEM analysis results for the related grafts, two middle rows show the displacement patterns of 16C/16R filaments graft and FEM analysis results for the associated grafts, and two last rows show DOEH analysis and acoustic behavior of new human temporalis fascia and human TM. The measurements at different frequencies are presented by four columns. The most correlated regions are also mentioned with dashed lines.

categories have nearly equal performance at frequencies less than 1000 Hz. Likewise, for displacement magnitudes at (3000 Hz), the correlation of FEM outputs to the human TM behavioral range is in a satisfying condition. Additionally, the distribution of color bar patterns for the FEM model is in a remarkable homogeneity, especially for the 80 to 100 dB sound pressure range. In contrast, this issue is not confirmed for temporalis fascia at this range where the color bar patterns of FEM models show no satisfying homogeneity. Even though the simple modal motion of DOEH at 0.4 kHz shows a distributed color bars mapping with maxima displacement overall sample surfaces, FEM analysis results for both architectural categories are in similar patterns at this frequency. These patterns slightly change at tested frequencies higher than 1 kHz. The acoustic performance of the (16C/16R) TM composite graft shows a simple movement pattern with the dominance of a lower mode of motion compared to the 8C/8R in PDMS-based TM graft. But the patterns resulted from the FEM analysis show good agreement to the human TM performance at (1000 Hz) where PDMS 3D printed TM graft cannot satisfy the motion pattern similarity. Asymmetric motion pattern of the temporalis fascia approximates the TM grafts pattern in DOEH results, but they are in a real difference in motion pattern comparison with FEM results. However,

observations show that compared to the human TM, the motion pattern for simulated models is symmetric in general.

In contrast, human TM's highly asymmetric motion patterns result from limited membrane displacement due to asymmetrically placed manubrium, umbo, and complicated irregular shape of TM in three dimensions. Thus, at frequencies (> 3000 Hz), the patterns of FEM models show absolute sameness in comparison with temporalis fascia and 3D printed TM graft patterns. The samples' complex motion patterns at frequencies (> 1 kHz) can be seen as concentric ring color bars arrangement for the exhibition of local maxima and minima displacements. The ring-shaped bars in color mapping related to FEM patterns are distributed in a very relative homogeneity in comparison with human TM at (< 3000 Hz). In other words, the symmetrical pattern of the FEM models is close to the human TM to exhibit local maxima and minima displacements of motion. With a similar analysis for PLA-based printed grafts, results for displacement magnitudes can be explained as shown in Figure 6.

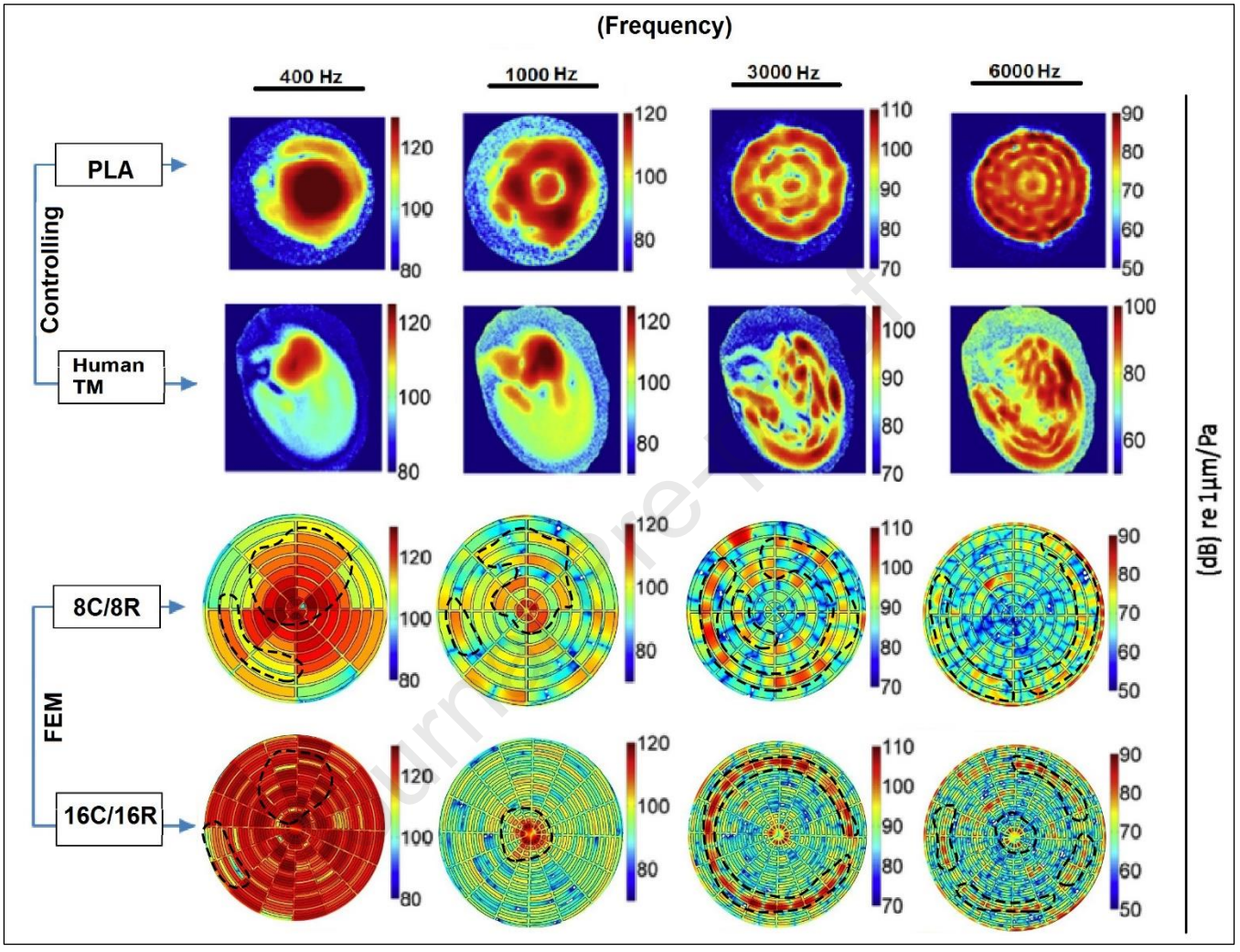

Fig. 6. Analysis results as normalized displacement by sound pressure at dB re 1 µm/Pa units for PLA-based samples to provide data for comparative analysis with DOEH fringe patterns of printed tympanic membrane composite grafts (reprinted and modified from [21] with permission from Elsevier), and FEM models controlled with human tympanic membrane: Top two rows show the displacement patterns of the visible 9 mm diameter section of an 8C/8R graft and sheet of fresh human TM with intact middle ear for control, two last rows show acoustic analysis results of 8C/8R and 16C/16R graft with FEM simulation based on PLA material. The measurements at different frequencies are presented by four columns. The most correlated regions are also mentioned with dashed lines.

The acoustic behavior of TM graft at 1000 Hz frequency is in a satisfying correlation with FEM models but the propagation of color bar patterns for the FEM model is in an adaptive shape close to the human TM pattern. At frequencies (< 3000 Hz), homogeneity in the acoustic performance of FEM and 3D printed TM grafts is in satisfying condition, where the FEM pattern shows a good correlation with the human TM behavior at this range. As it can be seen, the human TM has a slight change in dBs moving from (3000 Hz to 6000 Hz) frequencies but this is observed for the FEM model in the 90-100 dB range. Noteworthy, this issue is not observed at PDMS- based samples in the same range of sound pressure. In a similar way, motion patterns for PCL-based TM composite grafts are presented in Figure 7. The acoustic performance of these grafts is in the same pattern seen for PLA-based samples at 400 Hz and 1000 Hz. Observations for these patterns are recorded with a local displacement difference with the FEM model at 1000 Hz. The PCL-based TM graft is in a high maximum magnitude at 1000 Hz with a big difference of human TM in a range between 100 to 120 dB. The motion pattern of the FEM model shows a good correlation with the human TM motion pattern in this domain. At higher frequencies of more than 3000 Hz, similar to the two other materials, color visual bar patterns exhibiting the maxima magnitude of displacements by FEM models are in a concentric distribution of ring-shaped color bar identical to the human TM. Also, for frequencies (<1000 Hz), the performance of all the materials becomes more complex, with multiple areas of maximal displacement separated by regions of reduced displacement in DOEH motion patterns. The FEM analysis results of samples confirm this with exhibition variety in the locations and number of the maximal displacement magnitudes and complicated motion patterns. Increasing the number of ring-shaped color bars with increasing frequency in each material is the other correlation according to experimental tests.

In general, motion patterns of simulated grafts recorded from the vibro-acoustic analysis are in a satisfying correlation with patterns of 3D printed grafts. In contrast, some differences in the number and spacing of local displacement maxima are observed as well. But more symmetrical performances are related to FEM models created by PLA and PCL materials. It is also worth mentioning that the statistically significant inverse correlation between frequency and maximum displacement is observable in FEM models. Although the surface motion of the members is affected by several

geometrical and material properties, this feature could be improved by some optimization techniques.

3.2.2. Surface velocity of samples

It is discussed before that the motion patterns for comparative analysis of local displacement on sample surfaces are obtained from the DOEH test whit technical limitations in frequency resolution. To tackle this, at the frequency range of 100 Hz to 10 kHz, LDV was employed to observe the sound-induced velocity changes in the center of the samples. As mentioned before, Figure 4a shows the mean of velocity measurements normalized by sound pressure for multiple experimental tests on samples. Also, the peak in the normalized velocity patterns for all materials is collected in Table 3.

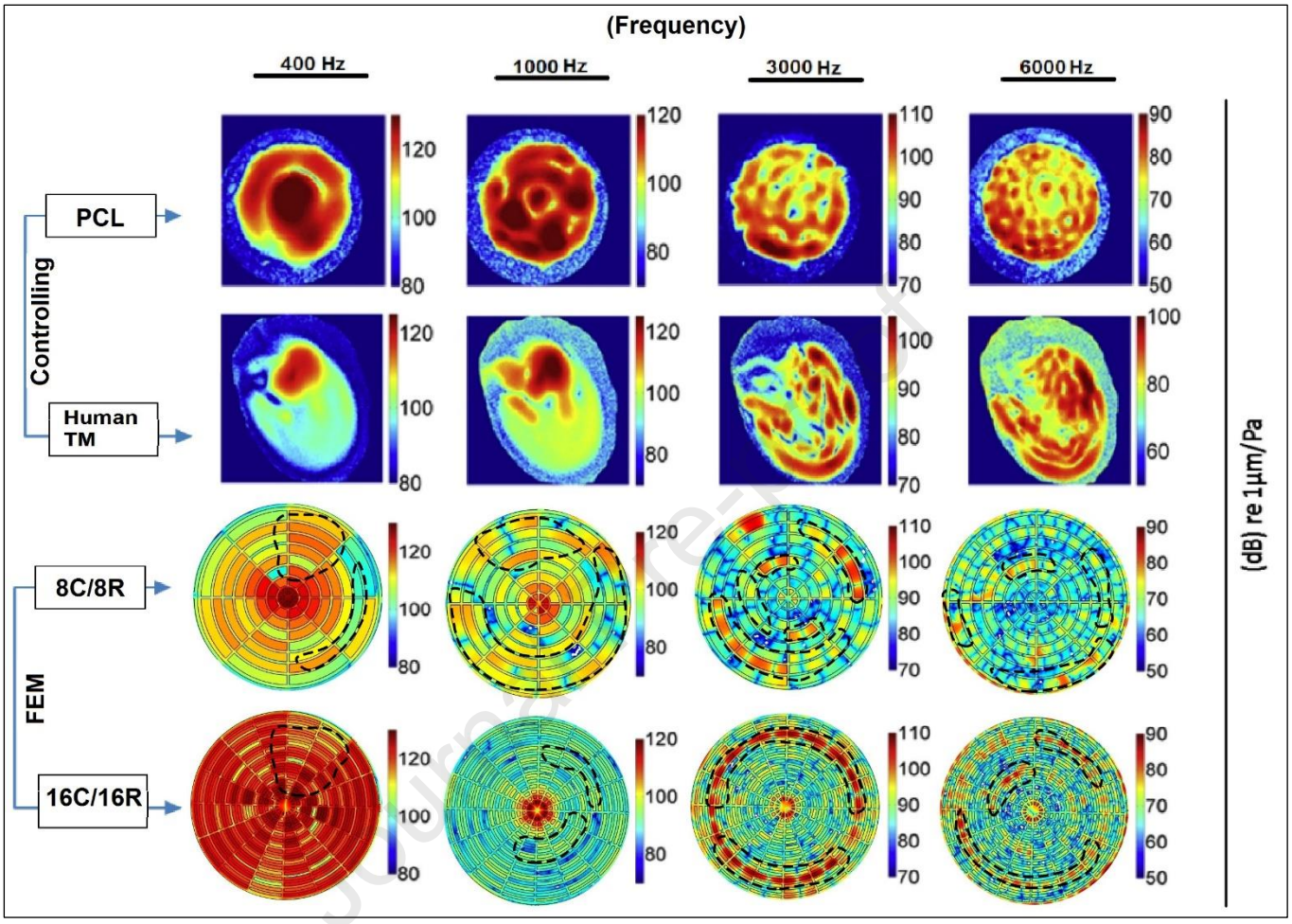

Fig. 7. Analysis results as normalized displacement by sound pressure at dB re 1 µm/Pa units for PCL-based samples to provide data for comparative analysis with DOEH fringe patterns of printed tympanic membrane composite grafts (reprinted and modified from [21] with permission from Elsevier), and FEM models controlled with human tympanic membrane: Top two rows show the displacement patterns of the visible 9 mm diameter section of an 8C/8R graft and sheet of fresh human TM with intact middle ear for control, two last rows show acoustic analysis results of 8C/8R and 16C/16R graft with FEM simulation based on PCL material. The measurements at different frequencies are presented by four columns.

Table 3
Peaks in normalized velocity patterns of printed TM grafts recorded from LDV

Filament categories of 3D Printed TM Grafts	Peak of Normalized Velocity (m/s /Pa)		
	PDMS	PLA	PCL
8C/8R	0.040	0.065	0.050
16C/16R	0.010	0.050	0.010

Three different TM composite grafts printed in the 8C/8R configuration created from PDMS, PLA, and PCL materials are indicated. Again, the lowest frequencies exhibit the highest velocity with a peak around 140 Hz. Likewise, it is observed that PDMS composite grafts exhibit the lowest velocities. Figure 4b shows the recorded statistical graphs of normalized velocity measurements for PDMS, PLA, and PCL- based TM composite grafts obtained from FEM analysis. To validate the obtained data from FEM analysis for the surface velocity of the grafts, a comparative analysis with the velocity patterns of human fascia, and the other grafts (shown as Figure 4a) is carried out. The more symmetric pattern is related to PLA-based grafts, wherein PDMS and PCL have approximately identical patterns. At frequencies (less than 1 kHz), umbo shows a lower velocity than FEM grafts velocity patterns. In general, the correlation in the average velocity of all FEM models is confirmed. The approximate and promising homogeneity of coincident peaks in normalized velocity patterns resulting from FEM analysis and LDV tests can be inferred from Table 3 and Figure 4b. There are approximate agreements between peaks of velocities in recorded patterns from LDV with the same data observed from FEM analysis. Additionally, a clear correlation is observed for PLA material with an approximate amount of (0.005 m/s / Pa) for 16C/16R grafts and (0.05 m/s / Pa) for 8C/8R grafts to both experimental and FEM analysis results. Slightly less motion at low frequencies for 16C/16R grafts comparing with 8C/8R grafts is another good correlation of FEM analysis and experimental results. But, in a general view, it can be concluded that the filament count of the graft scaffolds has no significant effect on velocity measurement patterns. However, with a comparative analysis between existing data, (Figure 4a, and Table 3), and results obtained from the computational analysis (see Figure 4a), the shape of the patterns and location of local peaks in velocity can be found in a satisfying correlation.

3.2.3. Summary of the FEM models and human TM correlation results

On the other hand, studies on the results obtained for simulated TM grafts for validation by the acoustic performance of the human fresh TM are performed. At lower frequencies (between 400 Hz and 1 kHz), all (8C/8R) polymeric models are in a good correlation in acoustic behavior with human TM. For PDMS-based models, this issue is observable for a high range of surface areas. But for frequencies, more than (3000 Hz) the scenario is changed. Models in both lattice patterns can satisfy the performance similarities where more agreements are observed in the (16C/16R) lattice patterns for all materials. Again, the PDMS-based (16C/16R) models show the highest correlation in acoustic performance in comparison with the human TM responses. The flutings in the color map outputs for PDMS-based grafts are mentioned with dashed lines in Figure 5 can demonstrate this result. For models simulated with PLA and PCL materials, the array of the dashed line for mentioning the correlated zones is not close to the similar color-based index in the human TM but in general FEM models replicate the acoustic performance in a good correlation. However, the exciting differences between the observations of the FEM analysis and experimental analysis are undeniable. These differences have resulted from parameters involved in the modeling, printing process, and experimental analysis procedures. Hence, boundary condition asymmetry in the experimental study, the imaging processing of results, and the existence of gel in all areas of the models may be some probable factors.

4. Discussion and Summary

Numerical and multiphysics simulation of the 3D printed TM grafts has been performed in this research. Some highlighted agreements between experimental studies conducted by [21], existing data for control, and vibro-acoustic FEM simulation and analysis are listed as follows:

1. 3D printed PDMS material-based grafts show a high degree of symmetry in radial color bars mapping at the higher frequencies.
2. Geometrical feature of the number of filaments has no real impact on the motion pattern, especially at frequencies higher than 1000 Hz.
3. At frequencies higher than 3000 Hz, more symmetry between obtained results from FEM, human TM, and temporalis fascia is observed for 8C/8R category samples.
4. For 80 to 100 dB sound pressure range, the displacement magnitudes recorded for FEM models are in a remarkable homogeneity with human TM.
5. FEM analysis results for the acoustic performance of 16C/16R TM composite graft show substantial equivalence to the human TM at 1000 Hz.
6. Unlike temporalis fascia, there is a clear correlation between motion patterns of FEM models and human TM.
7. FEM displacement patterns show a good relationship with temporalis fascia and TM graft patterns at frequencies higher than 3000 Hz.
8. According to complex motion patterns, a satisfying correlation is observed between FEM results and human TM motion patterns at frequencies (< 3000 Hz).
9. According to the acoustic behavior of PLA-based printed TM grafts at 1000 Hz frequency, the concentric color bar arrangement for FE models and human TM is in a significant correlation.
10. PCL-based grafts have the same performance as the PLA-based samples at 400 Hz and 1000 Hz.
11. In a range between 100 and 120 dB, PCL-based FEM models correlate with human TM motion patterns.
12. In parallel with ODEH results, at frequencies <1000 Hz, the performance of all the materials becomes more complex.
13. Increasing the number of ring-shaped color bars with increasing frequency in each material is observed in FEM model patterns.
14. FEM models exhibit the highest velocity at the lowest frequencies.
15. At frequencies less than 1 kHz, umbo shows a lower velocity than FEM grafts velocity patterns.
16. Demonstration of good homogeneity of coincident peaks in normalized velocity patterns resulted from FEM analysis and LDV tests is observed.
17. In general, the adjustment of velocity patterns and location of local peaks are in an acceptable correlation considering both FE models and experimental test results.

Consequently, despite similarities in the acoustic performance between the simulated models and the printed grafts, there are also differences because of some involving factors such as the structural lattice pattern, material properties, and differences in the modeling and experimental testing conditions and assumptions. But a general correlation is observed between the acoustic performance of the FEM simulated grafts, experimental tests for printed grafts, and fresh human TM.

However, the simulation techniques such as FEM have appeared as an excellent opportunity for decreasing costs and performing time in a wide range of experimental studies. This may reduce the existing gaps between practice and theoretical studies before doing any trial and error. Sometimes carrying out computer aid analysis and tests for finding the more suitable outcomes of biomedical engineering projects could shorten the design and pre-studying steps. In this paper, numerical simulations of the designed and 3D printed TM grafts are performed to demonstrate the multiphysical feasibility of the experimentally validated grafts. The highlighted aim of the study is to find a low-cost method for optimization and improve the quality of the 3D printing technique in the fabrication of TM grafts. The comparative analysis between experimental and simulation results shows that even though vibro-acoustic simulation is an excellent opportunity for studying and the design procedure of TM grafts, considering all practical aspects of fabrication of more feasible grafts is essential.

5. Conclusion

This study demonstrated a numerical simulation of the in-vitro evaluated and experimentally tested 3D printed TM grafts. After carrying out the vibro-acoustic analysis with FEM dynamic modeling in COMSOL Multiphysics Software, obtained results were used in comparative and statistical analysis with experimental results taken from [21]. Observations showed that the printed TM grafts are biomechanically qualified for potential use in the tympanoplasty procedure. Besides, detecting possible clinical and biomechanical limits, such as graft failure due to chronic negative pressures in the middle ear, needs further studies. Even though studying for geometrically optimized grafts is necessary, using bio-inspired materials and structural features may help to obtain more feasible and clinically applicable scaffolds [38].

References

[1] G. Volandri, F. Di Puccio, P. Forte, C. Carmignani, Biomechanics of the tympanic membrane, J. Biomech. 44 (2011) 1219–1236.

[2] D.H. McFarland, Netter's Atlas of Anatomy for Speech, Swallowing, and Hearing-E-Book, Elsevier Health Sciences, 2014.

[3] D. Strens, G. Knerer, I. Van Vlaenderen, I.J.M. Dhooge, A pilot cost-of-illness study on long-term complications/sequelae of AOM., B-ENT. 8 (2012) 153.

[4] J. Liang, K.D. Smith, R.Z. Gan, H. Lu, The effect of blast overpressure on the mechanical properties of the human tympanic membrane, J. Mech. Behav. Biomed. Mater. 100 (2019) 103368.

[5] B.M. Teh, R.J. Marano, Y. Shen, P.L. Friedland, R.J. Dilley, M.D. Atlas, Tissue engineering of the tympanic membrane, Tissue Eng. Part B Rev. 19 (2013) 116–132.

[6] Q. Zhang, Z. Lou, Impact of basic fibroblast growth factor on healing of tympanic membrane perforations due to direct penetrating trauma: a prospective non-blinded/controlled study, Clin. Otolaryngol. 37 (2012) 446–451.

[7] R. Ghassemifar, S. Redmond, Zainuddin, T. V Chirila, Advancing towards a tissue-engineered tympanic membrane: silk fibroin as a substratum for growing human eardrum keratinocytes, J. Biomater. Appl. 24 (2010) 591–606.

[8] M.A. Villar-Fernandez, J.A. Lopez-Escamez, Outlook for tissue engineering of the tympanic membrane, Audiol. Res. 5 (2015) 9–19.

[9] B. Levin, R. Rajkhowa, S.L. Redmond, M.D. Atlas, Grafts in myringoplasty: utilizing a silk fibroin scaffold as a novel device, Expert Rev. Med. Devices. 6 (2009) 653–664.

[10] R. Di Gesù, A.P. Acharya, I. Jacobs, R. Gottardi, 3D printing for tissue engineering in otolaryngology, Connect. Tissue Res. 61 (2020) 117–136.

[11] F.S. França, M.G. dos Santos, J.P. Prestes, B. Alcântara, M.F. Borges, P. Pranke, Bioprinting: A promising approach for tissue regeneration, Bioprinting. (2021) e00130.

[12] M. Askari, M.A. Naniz, M. Kouhi, A. Saberi, A. Zolfagharian, M. Bodaghi, Recent progress in extrusion 3D bioprinting of hydrogel biomaterials for tissue regeneration: A comprehensive review with focus on advanced fabrication techniques, Biomater. Sci. 9 (2021) 535–573.

[13] A. Zolfagharian, H.R. Jarrah, M. Bodaghi, 4D Printing Classroom in Modern Interactive Learning Environments, Bioprinting. 24 (2021) e00169.

[14] M. Aleemardani, Z. Bagher, M. Farhadi, H. Chahsetareh, R. Najafi, B. Eftekhari, A. Seifalian, Can Tissue Engineering Bring Hope to the Development of Human Tympanic Membrane?, Tissue Eng. Part B Rev. (2021).

[15] C.-Y. Kuo, E. Wilson, A. Fuson, N. Gandhi, R. Monfaredi, A. Jenkins, M. Romero, M. Santoro, J.P. Fisher, K. Cleary, Repair of tympanic membrane perforations with customized bioprinted ear grafts using chinchilla models, Tissue Eng. Part A. 24 (2018) 527–535.

[16] N. Zhong, X. Zhao, 3D printing for clinical application in otorhinolaryngology, Eur. Arch. Oto-Rhino-Laryngology. 274 (2017) 4079–4089.

[17] L. Li, W. Zhang, M. Huang, J. Li, J. Chen, M. Zhou, J. He, Preparation of gelatin/genipin nanofibrous membrane for tympanic member repair, J. Biomater. Sci. Polym. Ed. 29 (2018) 2154–2167.

[18] Z. Yang, X. Chen, F. Ye, Y. Huang, X. Wu, C. Wu, Comparison of endoscopic type I tympanoplasty with and without assistance of customized 3D-printed guiding template for tympanic membrane, Am. J. Otolaryngol. 42 (2021) 103042. https://doi.org/https://doi.org/10.1016/j.amjoto.2021.103042.

[19] E. Ilhan, S. Ulag, A. Sahin, B.K. Yilmaz, N. Ekren, O. Kilic, M. Sengor, D.M. Kalaskar, F.N. Oktar, O. Gunduz, Fabrication of tissue-engineered tympanic membrane patches using 3D-Printing technology, J. Mech. Behav. Biomed. Mater. 114 (2021) 104219.

[20] S.H. Kim, H.J. Lee, J.-C. Yoo, H.J. Park, J.Y. Jeong, Y.B. Seo, M.T. Sultan, S.H. Kim, O.J. Lee, C.H. Park, Novel transparent collagen film patch derived from duck's feet for tympanic membrane perforation, J. Biomater. Sci. Polym. Ed. 29 (2018) 997–1010.

[21] E.D. Kozin, N.L. Black, J.T. Cheng, M.J. Cotler, M.J. McKenna, D.J. Lee, J.A. Lewis, J.J. Rosowski, A.K. Remenschneider, Design, fabrication, and in vitro testing of novel three-dimensionally printed tympanic membrane grafts, Hear. Res. 340 (2016) 191–203.

[22] K.C.R. Kolan, J.A. Semon, A.T. Bindbeutel, D.E. Day, M.C. Leu, Bioprinting with bioactive glass loaded polylactic acid composite and human adipose stem cells, Bioprinting. 18 (2020) e00075.

[23] S. Liu, S. Qin, M. He, D. Zhou, Q. Qin, H. Wang, Current applications of poly (lactic acid) composites in tissue engineering and drug delivery, Compos. Part B Eng. (2020) 108238.

[24] D.L. Schulte, C.L. Driscoll, T.J. McDonald, G.W. Facer, C.W. Beatty, Irradiated rib cartilage graft for reconstruction of the tympanic membrane: preliminary results., Am. J. Otol. 19 (1998) 141–144.

[25] M.S. Lopes, A.L. Jardini, R. Maciel Filho, Poly (lactic acid) production for tissue engineering applications, Procedia Eng. 42 (2012) 1402–1413.

[26] M.O. Aydogdu, E.T. Oner, N. Ekren, G. Erdemir, S.E. Kuruca, E. Yuca, M.S. Bostan, M.S. Eroglu, F. Ikram, M. Uzun, Comparative characterization of the hydrogel added PLA/β-TCP scaffolds produced by 3D bioprinting, Bioprinting. 13 (2019) e00046.

[27] A. Victor, J.E. Ribeiro, F.F. Araújo, Study of PDMS characterization and its applications in biomedicine: A review, J. Mech. Eng. Biomech. 4 (2019) 1–9.

[28] G. Xu, Z. Ni, X. Chen, J. Tu, X. Guo, H. Bruus, D. Zhang, Acoustic Characterization of Polydimethylsiloxane for Microscale Acoustofluidics, Phys. Rev. Appl. 13 (2020) 54069.

[29] P.R.L. Nalesso, W. Wang, Y. Hou, L. Bagne, A.T. Pereira, J.V. Helaehil, T.A.M. de Andrade, G.B. Chiarotto, P. Bártolo, G.F. Caetano, In vivo investigation of 3D printed polycaprolactone/graphene electro-active bone scaffolds, Bioprinting. 24 (2021) e00164.

[30] S. Ramasamy, P. Davoodi, S. Vijayavenkataraman, J.H. Teoh, A.M. Thamizhchelvan, K.S. Robinson, B. Wu, J.Y.H. Fuh, T. DiColandrea, H. Zhao, Optimized construction of a full thickness human skin equivalent using 3D bioprinting and a PCL/collagen dermal scaffold, Bioprinting. 21 (2021) e00123.

[31] M. Mirbagheri, D. Mohebbi-Kalhori, N. Jirofti, Evaluation of mechanical properties and medical applications of polycaprolactone small diameter artificial blood vessels, Int. J. Basic Sci. Med. 2 (2017) 58–70.

[32] M.A. Elsawy, K.-H. Kim, J.-W. Park, A. Deep, Hydrolytic degradation of polylactic acid (PLA) and its composites, Renew. Sustain. Energy Rev. 79 (2017) 1346–1352.

[33] D. Rahmatabadi, A. Aminzadeh, M. Aberoumand, M. Moradi, Mechanical Characterization of Fused Deposition Modeling (FDM) 3D Printed Parts, Fused Depos. Model. Based 3D Print. (2021) 131.

[34] M. Aberoumand, D. Rahmatabadi, A. Aminzadeh, M. Moradi, 4D Printing by Fused Deposition Modeling (FDM), Fused Depos. Model. Based 3D Print. (2021) 377.

[35] M. Guvendiren, J. Molde, R.M.D. Soares, J. Kohn, Designing biomaterials for 3D printing, ACS Biomater. Sci. Eng. 2 (2016) 1679–1693.

[36] R. Baptista, M. Guedes, M.F.C. Pereira, A. Maurício, H. Carrelo, T. Cidade, On the effect of design and fabrication parameters on mechanical performance of 3D printed PLA scaffolds, Bioprinting. 20 (2020) e00096.

[37] H.O. Agu, A. Hameed, G.J. Appleby-Thomas, D.C. Wood, The dynamic response of dense 3 dimensionally printed polylactic acid, J. Dyn. Behav. Mater. 5 (2019) 377–386.

[38] A.A. Rostam-Alilou, H. Jafari, A. Zolfagharian, A. Serjouei, M. Bodaghi, Using Fibrincollagen Composite Hydrogel and Silk for Bio-inspired Design of Tympanic Membrane Grafts: A Vibro-acoustic Analysis, Compos. Part C Open Access. (2021) 100205. https://doi.org/https://doi.org/10.1016/j.jcomc.2021.100205.

[39] F. Gentil, C. Garbe, M. Parente, P. Martins, C. Santos, E. Almeida, R.N. Jorge, The biomechanical effects of stapes replacement by prostheses on the tympano-ossicular chain, Int. j. Numer. Method. Biomed. Eng. 30 (2014) 1409–1420.

[40] M.P. Wylie, G.B. McGuinness, G.P. Gavin, A linear finite element acoustic fluid–structure model of ultrasonic angioplasty in vivo, Int. j. Numer. Method. Biomed. Eng. 26 (2010) 828–842.

[41] E. Boccia, A. Gizzi, C. Cherubini, M.G.C. Nestola, S. Filippi, Viscoelastic computational modeling of the human head-neck system: Eigenfrequencies and time-dependent analysis, Int. j. Numer. Method. Biomed. Eng. 34 (2018) e2900.

[42] S. Sathyan, U. Aydin, A. Belahcen, Acoustic noise computation of electrical motors using the boundary element method, Energies. 13 (2020) 245.

We confirm that there are no known conflicts of interest associated with this publication and there has been no significant financial support for this work that could have influenced its outcome.

Declaration of interests

☒The authors declare that they have no known competing financial interests or personal relationships that could have appeared to influence the work reported in this paper.

☐The authors declare the following financial interests/personal relationships which may be considered as potential competing interests: